RSC Advances

ROYAL SOCIETY OF CHEMISTRY

www.rsc.org/advances

RSC Advances

RSCPublishing

ARTICLE

Oxygen adsorption properties on Palladium promoted $La_{1-x}Sr_xMnO_3$ solid oxide fuel cell cathode

Cite this: DOI: 10.1039/x0xx00000x

Lichao Jia,[a] Kai Li,[a] Dong Yan,[a] Xin Wang,[a] Bo Chi,[a] Jian Pu,[a] Li Jian*[a] and Songliu Yuan[b]

Received 00th January 2012,

Accepted 00th January 2012

DOI: 10.1039/x0xx00000x

www.rsc.org/

Surface reaction of O_2 molecules on Sr-doped $LaMnO_3$ (LSM) cathode and Pd impregnated LSM cathode is investigated by the first principles method. Tetrahedral Pd_4 cluster is used to simulate the Pd particles on the LSM surface. The calculated adsorption energies demonstrate that the pre-adsorbed Pd facilitates O_2 adsorption on the surface. The bond length of adsorbed O_2 species and corresponding dissociation energies indicate that O_2 molecule on the Pd/LSM cathode surface can be dissociated more easily than that on pure LSM surface. The pre-adsorbed Pd (atom and cluster) can serve as an active center on the surface and enhance the electron transference properties during the oxygen reduction reactions.

Introduction

Sr-doped $LaMnO_3$ ($La_{1-x}Sr_xMnO_3$, LSM) has been used as cathode of high temperature solid oxide fuel cells (SOFCs) for its excellent chemistry compatibility with common electrolyte Y_2O_3 stabilized Zr_2O_3 (YSZ), good stability and oxygen reduction catalytic activity at 1000 °C [1-3]. However, the polarization loss of LSM cathode sharply increases with the decrease of the working temperature [4], leading to a poor performance of the cathode material for intermediate temperature (IT) SOFCs.

Great efforts [5-7] have been devoted to improve the performance of LSM cathode, such as compositing with YSZ [8] or Gd doped CeO_2 (GDC) [9, 10] electrolyte to increase the triple phase boundary (TPB), and B-site doping with different ions [11] to enhance the ionic conduction ability. Besides, the addition of noble metals [12, 13] (Pt, Pd, Ag, etc) into the cathode is expected to improve their electro-catalytic activity. Liang [14] reported that Pd impregnation in the LSM-YSZ porous structure significantly decreased cathode polarization resistance at temperatures between 600 and 850 °C, and the maximum power density of this kind of single cells could be up to 1.42 $W\cdot cm^{-2}$ (at 750 °C). Nevertheless, the promotion mechanism of Pd in the LSM cathode is still unclear and needs to be further explored.

The cathodic reaction is a multi-step chemical reaction, among which the surface reaction is found to determine the cathode performance [15]. The oxygen adsorption on the cathode surface is the first step and also a critical step during the cathode reaction process. A fundamental understanding of the reaction mechanism is of great importance. Liu's group [16-18] has examined the interactions between oxygen molecules and the (100) surfaces of $LaMnO_3$ and $La_{0.5}Sr_{0.5}MnO_{2.75}$, using the first principles method. It is found that the introduction of Sr and the resulting oxygen vacancies can facilitate the oxygen adsorption and dissociation. Oxygen adsorption and diffusion in the common used LSM cathode have also been studied systemically by Kuklja[19, 20]. According to their results, oxygen reduction reaction mainly occurs on the MnO-terminated (100) surface and the surface migration of the adsorbed oxygen species is slower than that of surface O vacancies. Recently, Zhou et al [21] have investigated the oxygen adsorption Ag/LSM (001) surface and found that the pre-adsorbed Ag on LSM surface can facilitate the oxygen dissociative adsorption and strengthen its activity as SOFC cathode by acting as an active center at the surface. All the mentioned studies prove that the first principles method based on density functional theory (DFT) is effective to investigate the oxygen adsorption mechanism.

In the present paper, we report the oxygen adsorption on LSM and Pd (cluster and atom) pre-adsorbed LSM (100) surfaces using the first principles method. It is intended to obtain the promotion mechanism of Pd on the LSM cathode performance. The result of this study is crucial to discover the mechanism of cathodic oxygen reduction and beneficial to develop high performance cathode materials.

Calculation approaches

We carry out first principles calculations by using the Projector Augmented Wave (PAW) [22] pseudo potentials as implemented in the Vienna ab-initio Simulation Package (VASP) [23, 24]. The exchange correlation functional is treated within the Generalized Gradient Approximation (GGA) and parameterized by Perdew-Burke-Ernzerhofer (PBE) formula [25]. The Brillouin-zone integrations are approximated by using the special k-point sampling of Monhkorst-Pack scheme [26]. A cutoff energy of 400 eV and a mesh size of 4×4×1 are used for geometry optimization and electronic property calculations. Utilizing the block Davidson scheme, both the atomic positions and cell parameters are optimized to the level of the residual forces below 0.01 $eV\cdot A^{-1}$.

Since the $LaMnO_3$ based cathode material has a cubic structure under SOFC operating conditions [27], only the highly symmetric cubic perovskite structure of *Pm*3*m* is considered.

The calculated lattice parameter is 3.86 Å, which is in good agreement with the previous study (3.88 Å) [17] and similar to our previous result [28]. It is found that the (100) surface may be energetically the most stable among all the surface models, such as (100), (110) and (111). Thus we choose the (100) surface with LaO- and MnO-terminated layers to study the adsorption of O_2 molecules on $LaMnO_3$-based cathode materials. Although $LaMnO_3$ (100) plane is a polar plane, four-layer slab is good enough to model the surface, because the system can be stabilized by the polarity compensation mechanisms[29]. Thus, a four-layer slab of (100) surface of $LaMnO_3$ consisting of MnO- and LaO- planes is constructed with a 15 Å thick vacuum layer to prevent an interaction between the two surfaces, similar to the previous study [21] about the oxygen adsorption on the Ag/LSM cathode surface. When used as a cathode material, LSM contains typically ~20% Sr. To reduce the system size and the computation time, supercells with periodicity (2×2) are employed and one La atom in the topmost LaO plane is replaced by a Sr atom, constructing the LSM(100) model with Sr doping ratio x=0.25.

The adsorption energy (E_{ads}), which corresponds to the energy gain from the adsorption of an atom on the metal surface, was defined by

$$E_{ads} = E_{adsorbate+slab} - E_{slab} - E_{adsorbate} \qquad (1)$$

where $E_{adsorbate+slab}$ is the total energy of the adsorbed assembly, and E_{slab} and $E_{adsorbate}$ are total energies of the clean surface and the adsorbate, respectively.

The nudged elastic band (NEB) calculations have been successfully used to predict pathways for multi-step reactions. Therefore this method is adopted to calculate the O_2 dissociation energy (E_{dis}). For the calculations, the surface is fixed, while only the adsorbed oxygen species are displaced. We first find out the transition state during the dissociation process of the adsorbed O_2 using the NEB method [30, 31]. The energy difference between transition state and the initial state represents the value of the E_{dis}.

Results and discussion

O_2 adsorption on LSM (100) surface

Oxygen incorporation into crystals begins at surfaces. So we investigate O_2 adsorption on LSM (100) surface firstly. Coverage of 0.25 monolayers (ML) by placing an oxygen molecule on one of the four cations on the top layer is adopted. As a comparison, the adsorption on O site of the surface is also studied. The adsorption energy is a criterion to determine the stability of the adsorption. According to equation (1), a positive value of E_{ads} means that the process is endothermic, while a negative value represents the exothermic reaction and implies energetically favorable adsorption.

Since the effect of oxygen vacancies for O_2-LSM surface interaction has been well documented by many researchers [20, 32], and we aim to examine the effect of Pd nanoparticles on the surface. And only surfaces without oxygen vacancies are employed to conduct this study. Table 1 shows the O_2 adsorption energies on the various adsorption sites of the MnO- and La(Sr)O- terminated planes and the corresponding structural parameters are also listed in the table. It can be confirmed that O_2 cannot be adsorbed on the atop surface O atoms of both the MnO- and La(Sr)O- terminated planes. The most favorable oxygen adsorption sites are found to be atop surface Mn atoms on the MnO-terminated surface and atop surface La atoms on the La(Sr)O-terminated LSM (001) surface. However, the La(Sr)O-terminated (100) surface is not the desired termination because of its high oxygen vacancy formation energy and the Sr segregation. Previous studies [20] demonstrate that for ABO_3-type perovskite structure cathode, B cations have higher activity than A cations toward the oxygen reduction. Therefore, only MnO-terminated (100) surface is considered in the following study. The calculated bond length of O_2 molecule in equilibrium gas phase is 1.23 Å, slightly larger than experimental value of 1.21 Å. As can be seen from Fig. 1(a) and Table 1, after adsorbed on the atop Mn atom, this bond length is enlarged to 1.29 Å. The elongate bond length of the adsorbed O_2 species shows that the chemical interaction between the two O atoms is weakened and the adsorbed O_2 molecule has a high propensity to dissociate. The distance between the adsorbed O atom (the one near the surface, O_{near}) and the surface Mn is determined to be 1.89 Å, which is smaller than the sum of the radius of Mn^{3+}/Mn^{4-} and O^{2-}, demonstrating that Mn and O are strongly interacted and connected by a chemical bond.

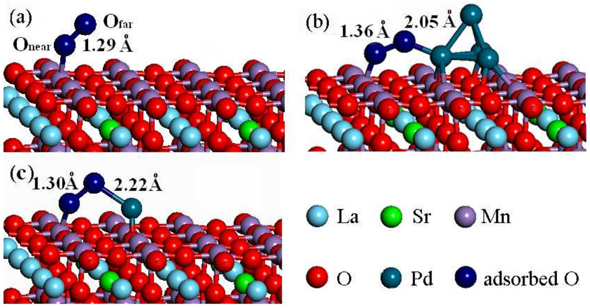

Fig. 1 The structures of O_2 adsorption on (a) clean LSM (100) surface; (b) Pd_4 cluster pre-adsorbed LSM (100) surface; (c) Pd atom pre-adsorbed LSM (100) surface.

Table 1 Calculated adsorption properties for O_2 molecule on LSM (100) surface

Site	E_{ads} (eV)	$d(O_{near}-O_{far})^a$ (Å)	$d(O_{near}-M_s)^b$ (Å)
MnO-			
O	0.16	1.24	3.27
Mn	-0.63	1.29	1.89
La(Sr)O-			
O	0.23	1.25	3.09
La	-0.42	1.28	2.39
Sr	0.39	1.27	2.64

[a] O_{near}, the adsorbed O atom nearest to the surface.
O_{far}, the adsorbed O atom far from the surface.
[b] M_s, the surface atom nearest to O_{near}.

Catalytic effect of Pd for O_2 adsorption on LSM (100) surface

Tetrahedral Pd_4 cluster is used to model the Pd particles on the LSM surface and the cluster size is determined based on previous study. Kalita et al. [33] have investigated the stability of Pd_n (n=1-7) clusters on the basis of structural and electronic properties by using the first principles method. And it is found that Pd_4 cluster has relatively high binding energy and the stability function shows higher relative stability of Pd_4 than the other clusters. The Pd_4 cluster is optimized in a 20 Å × 20 Å × 20 Å vacuum box, and then adsorbed onto the MnO-terminated LSM (100) surface to obtain the impregnated LSM cathode surface. Following, the O_2 adsorption properties are studied on such surface. A single Pd atom adsorbed on LSM (100) surface is also studied as comparison.

For Pd_4 cluster adsorbed system, Pd_4 cluster is adsorbed on the O site with an energy release of -2.49 eV. And the oxygen reduction reaction calculations are performed on the Pd_4 pre-adsorbed system. In Fig 1(b), we construct a surface model with O_2 molecule adsorbed on atop surface Mn or O site respectively, to simulate the TPB area for oxygen reduction reaction. The relative adsorption energy is calculated accordingly to Equation (1). The calculated adsorption energies and relative structural parameters are listed in Table 2. As can be seen, O_2 can be easily adsorbed on the atom surface Mn atom with the corresponding adsorption energy of -1.42 eV. The bond length of O_2 molecule increases from the equilibrium value 1.23 Å to 1.36 Å. The distance between O_{near} atom and surface Mn atom is 1.98 Å, and O_{far} (the adsorbed O atom far from the surface) is bonded to Pd with a chemical bond length of 2.05 Å. For the surface O site, after structure relaxation, the adsorbed O_2 molecule moves to surface Mn site, and the corresponding adsorption properties are very similar to that of Mn site case. This means that the introduction of Pd cluster can facilitate O_2 adsorption by increasing active site.

Table 2 Calculated adsorption properties for O_2 molecule on Pd_4 cluster pre-adsorbed LSM (100) surface.

Site	E_{ads} (eV)	$d(O_{near}\text{-}O_{far})$ (Å)	$d(O_{near}\text{-}Mn_s)^a$ (Å)	$d(O_{far}\text{-}Pd)$ (Å)
Mn	-1.43	1.36	1.98	2.05
O (Mn)	-1.42	1.36	1.99	2.06

[a] Mn_s represents the surface Mn atom nearest to O_{near}.

Table 3 Calculated adsorption properties for Pd atom on LSM (100) surface.

Site	E_{ads} (eV)	$d(Pd\text{-}M_s)$ (Å)
Mn	-1.22	2.37
O	-1.70	2.10

The Pd atom adsorption properties are investigated and the results are listed in Table 3. Two different sites on MnO-terminated LSM (100) surface are considered. It is found that Pd atom energetically prefers to adsorb at O site rather than at Mn site (-1.70 eV vs. -1.22 eV), which is similar to Ag adsorption on the LSM (100) surface [21]. For Pd pre-adsorbed system, O_2 molecule adsorption on Mn and O sites with pre-adsorbed Pd atom on O site is calculated. As can be seen from Table 4, the adsorption energies of the adsorption on Mn and O sites are -0.65 eV and -0.25 eV, respectively. With the addition of Pd atom, O_2 molecules which are far from the surface Mn atoms can be adsorbed on the Pd atoms. It can be concluded that the pre-adsorbed Pd atom can serve as an active center at the surface.

Table 4 Calculated adsorption properties for O_2 molecule on Pd atom pre-adsorbed LSM (100) surface.

Site	E_{ads} (eV)	$d(O_{near}\text{-}O_{far})$ (Å)	$d(O_{near}\text{-}Mn_s)$ (Å)	$d(O\text{-}Pd)^a$ (Å)
Mn	-0.65	1.30	1.96	2.22
O	-0.25	1.30	—	2.22

[a] d(O-Pd) corresponds to the distance between Pd and the nearest adsorbed O atom.

Discussion

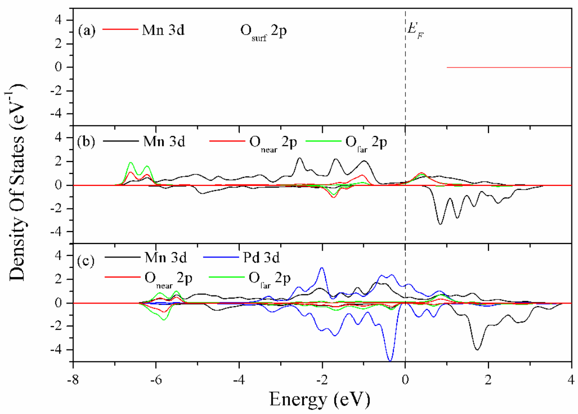

Fig. 2 PDOS for (a) clean LSM (100) surface; (2) O_2 absorbed LSM(100) surface; and (c) O_2 absorbed Pd_4 cluster pre-adsorbed LSM (100) surface. The Fermi Energy is set to be 0 and indicated by the vertical dashed line. Curves above and below the horizontal axis refer to the spin up and spin down PDOS, respectively.

Oxygen reduction reaction begins with the incorporation of O_2 onto the surface of SOFC cathode, which is very important to evaluate the electrochemical performance of certain materials. Comparing O_2 adsorption on pure LSM (100) surface and Pd_4 cluster or Pd atom pre-adsorption LSM (100) surface, it can be found that an important consequence of the adsorption is that bond length of adsorbed O_2 molecule increases from 1.28 Å to 1.36 Å. That is to say, pre-adsorbed Pd_4 cluster and Pd atom can facilitate the O_2 molecule dissociation to O atoms， which contributes to the subsequent surface oxygen diffusion. To validate this conclusion, the O_2 dissociation energy, which is one of key parameters besides E_{ads}, is also discussed in this study. The E_{dis} of the adsorbed O_2 is calculated. According to the results, after exothermic chemical adsorption, a barrier of 0.67 eV for the dissociation of the molecular oxygen species is needed to be overcome in the pure LSM (100) system with an energy difference of -0.87 eV between the final and initial state. The value of E_{dis} is lowered to be 0.52 eV in the Pd_4 cluster pre-adsorbed system, and the corresponding energy difference between the final and initial state is -1.43 eV. Thus the dissociation will be faster in Pd_4 cluster pre-adsorbed system than in pure LSM system. Furthermore, the more negative adsorption energy indicates that Pd is involved into the adsorption process and makes the adsorption easier and more stable.

To further understand the interactions between the adsorbates and surfaces, partial densities of states (PDOS) of O_2 adsorbed pure LSM (100) surface and Pd_4 cluster pre-adsorbed LSM (100) surface is calculated and plotted in Fig.2. As can be seen from Fig. 2(a), owing to the strong interaction between surface Mn and O by strong Mn-O chemical bond, Mn 3d and O 2p states cover a broad energy range of about 10 eV (from -7 eV to 3 eV). After O_2 adsorption, small overlap between Mn 3d and the adsorbed O 2p states appears at -6 eV ~ -7 eV (Fig. 2(b)), indicating the weak bonding between surface Mn and adsorbed O atoms. The two adsorbed O atoms are still bonded stably, which can be concluded from the similar shape at around -6.5 eV, -1.7 eV and 0.4 eV. Compared with Fig. 2(a), peaks of Mn 3d states above the Fermi Level would move to lower energy, which represents the electron transfer between surface Mn and the adsorbed species. For the Pd_4 pre-adsorbed system, the O-O interaction is weakened, as shown in Fig. 2(c). There is a weak overlap between Pd 3d states and the 2p states of adsorbed O atom, which is corresponding to the Pd-O_{far} bond. A considerable density of states appears around the Fermi level, and thus the transference of electrons will be easier than that in the system with Pd, resulting in a better electrochemical activity.

Conclusions

In summary, first-principles density functional theory calculations are performed to investigate the promotion mechanism of Pd on the LSM cathode performance. Surface reactions are concerned and the following conclusions can be made:

(1) Calculated adsorption energies suggest that O_2 molecules are preferentially adsorbed on the surface Mn site rather than O site of clean LSM (100) surface, while both Mn site and O site are active for O_2 adsorption on Pd_4 cluster pre-adsorbed LSM (100) surface.

(2) The lowest O_2 adsorption energy in clean LSM (100) system is determined to be -0.63 eV, and -1.43 eV in the Pd containing surface. The energy difference indicates that the addition of Pd makes the adsorption easier and more stable.

(3) The predicted bond length of O_2 molecule after adsorption shows that the adsorbed O_2 species on the Pd_4 cluster pre-adsorbed surface can be dissociated easier than that on the clean surface, which is validated by the calculated dissociation energy.

Acknowledgements

This research was financially supported by National Natural Science Foundation of China (U1134001), National “863” project of China (2011AA050702) and China Postdoctoral Science Foundation (2012M521423).

Notes and references

[a] Center for Fuel Cell Innovation, School of Materials Science and Engineering, State Key Lab of Material Processing and Die & Mould Technology, Huazhong University of Science and Technology, Wuhan, 430074, China. E-mail: lijian@hust.edu.cn; Fax: +86-27-87558142; el: +86-27-87557694

[b] School of Physics, Huazhong University of Science and Technology, Wuhan, 430074, China

1 S.P. Jiang, Y.J. Leng, S.H. Chan and K.A. Khor, *Electrochem. Solid St.*, 2003, **6**, A67-A70.

2 C. Sun, R. Hui and J. Roller, *J. Solid State Electr.*, 2010, **14**, 1125-1144.

3 K. Katsiev, B. Yildiz, K. Balasubramaniam and P.A. Salvador, *Appl Phys Lett*, 2009, **95**, 092106.

4 C. Xia and M. Liu, *Adv Mater*, 2002, **14**, 521-523.

5 M. Balaguer, V.B. Vert, L. Navarrete and J.M. Serra, *J. Power Sources*, 2013, **223**, 214-220.

6 D. Ding, X. Li, S.Y. Lai, K. Gerdes and M. Liu, *Energ. Environ. Sci.*, 2014, **7**, 552-575.

7 M.J. Jørgensen and M. Mogensen, *J. Electrochem. Soc.*, 2001, **148**, A433-A442.

8 R. Antunes, J. Jewulski and T. Golec, *J. Fuel Cell Sci. Tech.*, 2014, **11**, 011007.

9 T. Klemenso, C. Chatzichristodoulou, J. Nielsen, F. Bozza, K. Thyden, R. Kiebach and S. Ramousse, *Solid State Ionics*, 2012, **224**, 21-31.

10 B. Ahmed, S. B. Lee, R.H. Song, J.W. Lee, T.H. Lim and S.J. Park, *J. Solid State Electr.*, **18**, 435-443.

11 J. Chen, F. Liang, D. Yan, J. Pu, B. Chi, S.P. Jiang and L. Jian, *J. Power Sources*, 2010, **195**, 5201-5205.

12 M. Mosialek, M. Przybyla, M. Tatko, P. Nowak, M. Dudek and M. Zimowska, *Arch. Metall. Mater.*, 2013, **58**, 1337-1340.

13 Z. Wang, C. Xu, Z. Lou, J. Qiao, B. Ren and K. Sun, *Int. J. Hydrogen Energ.*, 2013, **38**, 1074-1081.

14 F. Liang, J. Chen, S.P. Jiang, B. Chi, J. Pu and L. Jian, *Electrochem. Commun.*, 2009, **11**, 1048-1051.

15 J. Fleig, *Ann. Rev. Mater. Res.*, 2003, **33**, 361-382.

16 Y. Choi, M.C. Lin and M. Liu, *Angew. Chem. Int. Edit.*, 2007, **46**, 7214-7219.

17 Y. Choi, M.E. Lynch, M.C. Lin and M. Liu, *J. Phys. Chem. C*, 2009, **113**, 7290-7297.

18 Y. Choi, M.C. Lin and M. Liu, *J. Power Sources*, 2010, **195**, 1441-1445.

19 Y.A. Mastrikov, R. Merkle, E. Heifets, E.A. Kotomin and J. Maier, *J. Phys. Chem. C*, 2010, **114**, 3017-3027.

20 M.M. Kuklja, E.A. Kotomin, R. Merkle, Y.A. Mastrikov and J. Maier, *Phys. Chem. Chem. Phys.*, 2013, **15**, 5443-5471.

21 Y. Zhou, Z. Lü, B. Wei, X. Zhu, X. Huang, W. Jiang and W. Su, *J. Power Sources*, 2012, **209**, 158-162.

22 P.E. Blöchl, *Phys. Rev. B*, 1994, **50**, 17953-17979.

23 G. Kresse and J. Hafner, *Phys. Rev. B*, 1993, **47**, 558-561.

24 G. Kresse and J. Furthmüller, P *Phys. Rev. B*, 1996, **54**, 11169-11186.

25 J.P. Perdew, K. Burke and M. Ernzerhof, *Phys. Rev. Lett.*, 1996, **7**, 73865-3868.

26 H.J. Monkhorst and J.D. Pack, *Phys. Rev. B*, 1976, **13**, 5188-5192.

27 Y.A. Mastrikov, E. Heifets, E.A. Kotomin and J. Maier, *Surf. Sci.*, 2009, **603**, 326-335.

28 L. Jia, X. Wang, W. Li, K. Li, B. Chi, J. Pu, L. Jian and S. Yuan, *J. Power Sources*, 2014, **253**, 138-142.

29 B. E. Gaddy, E. A. Paisley, J. P. Maria and D. L. Irving, *Phys. Rev. B*, 2014, **90**, 125403.

30 G. Mills, H. Jönsson and G. Schenter, Surf. Sci., 1995, **324**, 305-337.

31 G. Henkelman, B.P. Uberuaga and H. Jönsson, *J. Chem. Phys*., 2000, **113**, 9901-9904.

32 Y. Choi, D.S. Mebane, M.C. Lin and M. Liu, *Chem. Mater*., 2007, **19**, 1690-1699.

33 B. Kalita and R.C. Deka, *J. Chem. Phys.*, 2007, **127**, 244306.